

## Green Synthesis of Silver Nanoparticles using *Lantana camara* Fresh Leaf Extract for Qualitative Detection of $\text{Hg}^{2+}$ , $\text{Cu}^{2+}$ , $\text{Pb}^{2+}$ , and $\text{Mn}^{2+}$ in Aqueous Solution

Henry Fonda Aritonang\*, Talita Kojong, Harry Koleangan, and Audy Denny Wuntu

Physical Chemistry Division, Faculty of Mathematics and Natural Sciences, Sam Ratulangi University,  
Jl. Kampus Unsrat Kleak, Manado 95115, Indonesia

\* **Corresponding author:**

tel: +62-431-827560

email: henryaritonang@unsrat.ac.id

Received: March 25, 2021

Accepted: June 22, 2021

DOI: 10.22146/ijc.64902

**Abstract:** This research was focused on the discovery of new environmentally friendly sensors based on nanoscale materials whose main purpose was to detect the presence of heavy metals in aqueous solutions. The environmentally friendly extracellular biosynthetic technique was applied to produce silver nanoparticles (AgNPs). The reducing agents used were distilled water and ethanol extract obtained from fresh leaves of *Lantana camara*. The silver-containing extracts (Ag-extract) were then used to detect the presence of  $\text{Hg}^{2+}$ ,  $\text{Cu}^{2+}$ ,  $\text{Pb}^{2+}$ , and  $\text{Mn}^{2+}$  in aqueous solutions by the colorimetric method using UV-visible spectroscopy. The colloidal synthesis of AgNPs was then monitored by the same method. The spectrum obtained showed peaks between 430 and 450 nm according to the Plasmon absorbance of AgNP. AgNPs' size and shape were characterized using the Transmission Electron Microscopy (TEM) technique, which showed the average size varies from 1.6 to 25 nm. The colorimetric data showed that Ag-extract, both of distilled water or ethanol solvents, was the best for detecting the presence of  $\text{Hg}^{2+}$  followed by  $\text{Mn}^{2+}$ . On the other hand, Ag-extract in distilled water cannot detect  $\text{Cu}^{2+}$ ,  $\text{Pb}^{2+}$ , and  $\text{Mn}^{2+}$  ions, while almost all Ag-extracts in ethanol solvents could identify the presence of these metals.

**Keywords:** green synthesis; silver nanoparticles; *Lantana camara* fresh leaf extract; qualitative detection; heavy metal ions

### ■ INTRODUCTION

Heavy metals in natural waters are usually present in small amounts, although many of them are toxic even at very low concentrations. Arsenic (As), lead (Pb), cadmium (Cd), copper (Cu), nickel (Ni), mercury (Hg), chromium (Cr), manganese (Mn), cobalt (Co), zinc (Zn), and selenium (Se) are among them [1-2]. Therefore, monitoring water quality is very important to evaluate water conditions.

Some of the most recent analytical methods commonly used to detect heavy metal ions are inductively coupled plasma-optical emission spectroscopy (ICP-OES) [3], inductively coupled plasma mass spectrometry (ICP-MS) [4], atomic absorption spectrometer (AAS) [5], cyclic voltammetry [6], graphite furnace atomic absorption spectrometer (GFAAS) [7] and X-ray fluorescence spectrometry [8]. The advantages of using these methods are that they have relatively wide

application, high sensitivity, high selectivity, and can be used to measure a relatively large number of elements. These techniques, however, require expensive types of equipment, complex analytical steps, and highly trained technicians [9-10]. Nanotechnology can be an alternative tool to replace these methods [11-12].

Nanoparticles have been widely used in various fields, such as surface plasmon resonance (SPR) [9] based on chemical sensors using colorimetry. This method is most commonly used in metal determination because it is relatively easy and readable for the human eye. Silver nanoparticles (AgNPs) are one of the best plasmonics that has been used in SPR-based nanosensors to detect various analytes, including metal ions, such as  $\text{Hg}^{2+}$ ,  $\text{Pb}^{2+}$ ,  $\text{Co}^{2+}$ ,  $\text{Cd}^{2+}$ , and  $\text{Cu}^{2+}$  [13]. In addition, AgNPs can also be used to enhance their role as metal ion sensors. The functionalization of AgNPs with guanine has been used as a  $\text{Ba}^{2+}$  ion sensor [14].

Likewise,  $Mn^{2+}$  and  $Cd^{2+}$  metal ions can be detected in water samples by functional AgNPs with sulfoanthranilic dithiocarbamate acid [15]. Timolol forms aggregate with AgNPs so that it can be detected in drug samples [16]. In addition, AgNPs can be used by two compounds at once, namely 6-mercaptopuronic acid and melamine, which can detect  $Cr^{3+}$  and  $Ba^{2+}$  ions [17], citrate and melamine, which act as ligands that can detect the presence of  $Cr^{3+}$  and  $Hg^{2+}$  ions in water samples [18], and trisodium citrate and L-cysteine which are used to detect  $Co^{2+}$  [19]. The development of chemical sensing procedures has been carried out by Amirjani and Fatmehsari [20] using the iPhone 4s camera to detect ammonia content in water samples.

Methods that have been used to produce AgNPs include chemical methods [21], electrochemistry [22], radiation [23], photochemical methods [24], Langmuir-Blodgett [25], and phytochemicals-based approaches [26]. The use of chemical methods involves toxic chemicals, such as reducing agents and capping agents that are not safe for the environment. Therefore, some researchers used green synthesis as an alternative method for synthesizing nanoparticles using microorganisms [27], enzymes [28], bacterial cellulose [29-30], and plant extracts [31-34].

Some green synthesis using plant extracts such as *Actinidia deliciosa* [16], *Impatiens balsamina* [31], *Lantana camara* L (*L. camara*) [31,35], *Astragalus tribuloides* [36], *Caralluma tuberculata* [37], *Tragopogon collinus* [38], and *Muntingia calabura* [39], have been reported. The extracts act as reducing and stabilizing agents [40].

In the manufacture of *Lantana camara* extract, water solvent was more widely used [31,35,41-42], and only a few studies reported the use of alcohol [35,43] or petroleum ether [44] solvents. However, the AgNPs produced were only tested for their antibacterial activity. In addition, information concerning the application of plant extracts containing AgNPs applied to detect the presence of heavy metals in aqueous solutions is still very limited, especially extracts produced from different solvents, namely water and ethanol.

Therefore, this study was aimed to synthesize AgNP by utilizing fresh leaf extracts from *L. camara*, which is extracted using distilled water and ethanol solvents. Furthermore, extracts from each solvent containing AgNPs were used to detect the presence of heavy metals in aqueous solutions.

## ■ EXPERIMENTAL SECTION

### Materials

All reagents used were analytic grade and without further purification. Ethanol, silver nitrate ( $AgNO_3$ ), mercury(II) chloride ( $HgCl_2$ ), copper(II) chloride dihydrate ( $CuCl_2 \cdot 2H_2O$ ), lead (II) nitrate ( $Pb(NO_3)_2$ ), and manganese(II) sulfate monohydrate ( $MnSO_4 \cdot H_2O$ ) were all purchased from Sigma-Aldrich in Indonesia with a purity of at least 99.5%. Fresh leaves of *L. camara* (Fig. 1) were harvested from around Sam Ratulangi University, Indonesia. Milli-Q water was used to prepare all aqueous solutions used in the experiment.

### Instrumentation

The instruments used were UV-Visible Spectrophotometer (Shimadzu UV-1800) and TEM (JEOL HT-7700).

### Procedure

The following procedure was used to obtain an aqueous extract of *L. camara* leaves. First, the leaves were thoroughly washed with distilled water and cut into small pieces. After that, 2.5 g of cut leaves were added to 25 mL of distilled water (W) in a 100 mL beaker and heated at 70 °C for 1.5 h. It was then allowed to cool and was filtered with Whatman No. 40 filter paper. The extract (W-extract) was consequently used as fresh material for the next step. A similar procedure, which was used for the preparation of the ethanol extract of *L. camara* leaves (E-extract). Both extracts (from those of water and ethanol) were then used to synthesize AgNPs.

Aqueous  $AgNO_3$  solutions, with concentrations of 1, 2, 3, 4, and 5 mM, were placed in Erlenmeyer flasks. Each solution was then placed in a 100 mL beaker containing an aqueous extract of *L. camara* with a ratio of  $AgNO_3$  solution:extract = 17:1 (v/v) (18 mL). After

that, the beaker is covered with aluminum foil. All mixtures were then stirred at 1500 rpm at 70 °C for 1 h. Subsequently, they were stored in a refrigerator for analysis with a UV-vis spectrophotometer to characterize the AgNPs and TEM to analyze the size of AgNPs. The same process was applied to the ethanol extracts from *L. camara* leaves. Each colloid produced from the two solvents was then labeled as W1, W2, W3, W4, W5, and E1, E2, E3, E4, and E5.

The colorimetric method, which utilizes AgNPs contained in extracts (Ag-extracts), has been widely used to detect heavy metals in aqueous solutions. In this study, heavy metal solutions were prepared using 1000 ppm  $\text{Hg}^{2+}$ ,  $\text{Cu}^{2+}$ ,  $\text{Pb}^{2+}$ , and  $\text{Mn}^{2+}$ , and 1 mL of each solution was added to 3 mL of Ag-extract. The color change of the solution was then observed and characterized by a UV-vis spectrophotometer in the range of 350–650 nm. All solutions in this experiment (AgNO<sub>3</sub>, Ag-extract, and Ag-extract-heavy metals) were characterized using the same method. Analysis of the size distribution of the AgNPs was carried out using the TEM (JEOL HT-7700) method, which was operated with a voltage acceleration of 120 kV. AgNPs' size was analyzed using ImageJ software for each TEM image. The histograms of the size distribution are established by the Origin software.

## ■ RESULTS AND DISCUSSION

### Profile of *L. camara* Fresh Leaf Extract

The same color, light brown, was observed for *L. camara* fresh leaf extracts from both solvents. However, after heating, the color became different, where the W-extract was dark brown while the E-extract was dark green (Fig. 1). It suggests that different solvents can dissolve

different components of secondary metabolites found in each sample.

### Synthesis of AgNPs

Similar to the initial extract, the color of the extract after the addition of the AgNO<sub>3</sub> solution was also changed, and the difference was quite significant, as shown in Fig. 2. The W-extract colors were darker than the E-extract colors.

In Fig. 2, it appears that each precursor concentration produced a different color. The higher the concentration of the Ag precursor, the brighter the color of the solution. The comparison of the leaf extracts colors from the two solvents showed that the W-extract solution was darker than the E-extract solution. These results also indicated that there were differences in the number of secondary metabolites found in each solution [45]. The difference in extract color before and after adding AgNO<sub>3</sub> solution also showed that Ag<sup>+</sup> was reduced. AgNP formation from Ag<sup>+</sup> ions started from chemical reactions in the presence of phytochemical compounds (flavonoids, terpenoids, steroids) found in *L. camara* leaves as reducing and stabilizing agents. Furthermore, the Ag<sup>+</sup> ion could interact with the –OH group, which was oxidized into the –CHO and –COOH

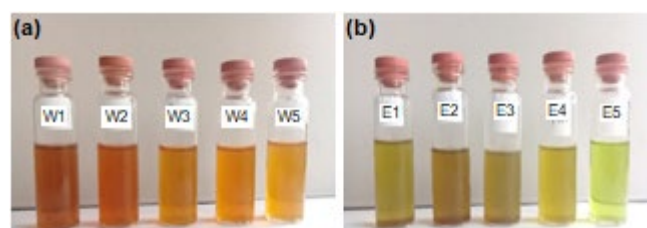


**Fig 2.** The color profile of Ag-extract at each concentration using (a) W and (b) E solvents

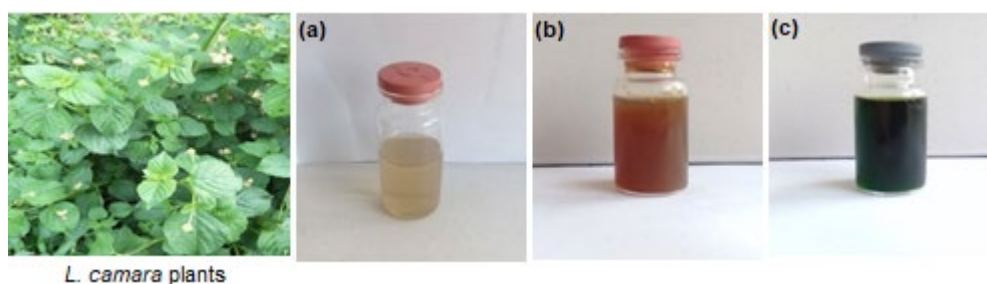


**Fig 1.** The color of fresh leaf extract from *L. camara*, (a) before and after heating with (b) W and (c) E solvents

groups and which were then reduced the  $\text{Ag}^+$  ions into AgNPs. In this case, the COOH group functions as a stabilizer for AgNPs [43].

### Analysis of AgNPs with UV-Vis Spectrophotometer

The Ag-extract solution was analyzed using a UV-Vis spectrophotometer to determine the characteristics of AgNPs based on the wavelength peak spectrum. The UV-Vis spectra of AgNPs in each solvent are in the range of 430 to 450 nm, as shown in Fig. 3. This range of maximum absorption peaks is similar to that reported by previous studies [20] and the broadening of peaks indicates that the particles were polydisperse. By careful observation, the absorption peak was around 440–430 nm, and the absorption location characteristic of the AgNPs peak was shifted towards a longer wavelength.

The UV-Vis spectrum in Fig. 3 shows that the  $\text{Ag}^+$  ion was reduced to  $\text{Ag}^0$ , which is confirmed by the absorbance peak, which occurs around 430–440 nm [46]. The higher the concentration of Ag, the higher the absorbance value. Thus, it seems that E solvent was able to dissolve chlorophyll from fresh *L. camara* leaf extract, which emerges in the spectrum of 620–680 nm (Fig. 3(b)).

### Surface morphology of AgNPs

The morphology, size, and surface shape of the biosynthesized AgNPs are visualized by TEM images. In the TEM image, as shown in Fig. 4(a, c, e, and g), nanoparticles generally show typical spherical and ellipsoidal morphology. The size distribution of biosynthesized nanoparticles was analyzed by ImageJ software. Based on the particle size distribution curve (Fig. 4(b, d), the average size of AgNPs at W1 and W5

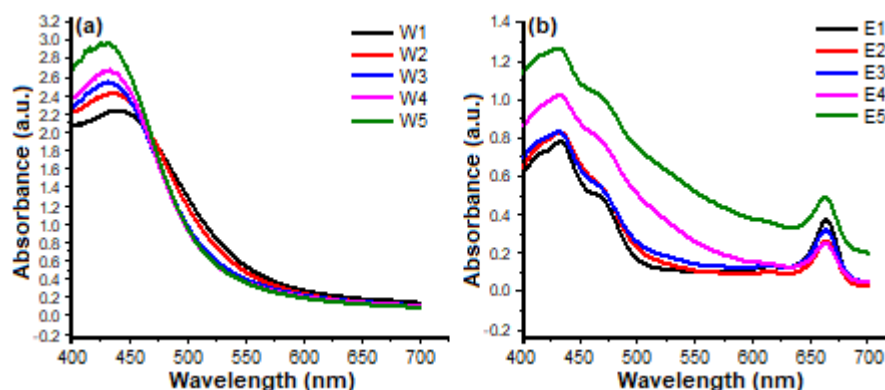


Fig 3. The UV-Vis spectrum of Ag-extract in (a) W and (b) E solvents, respectively

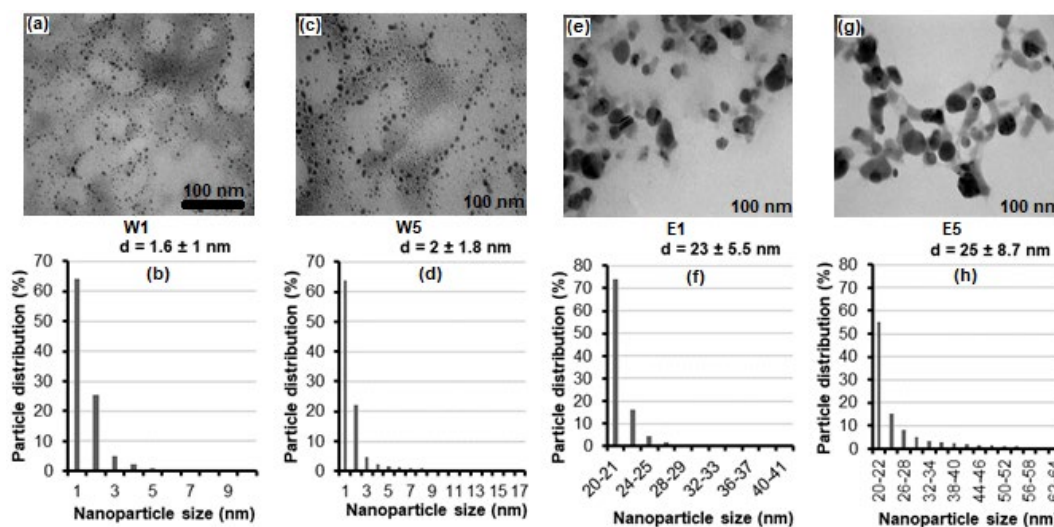


Fig 4. TEM image (a, c, e, g) and size distribution (b, d, f, h) of AgNPs produced from W1 (a, b), W5 (c, d), E1 (e, f), and E5 (g, h), respectively

were  $1.6 \pm 1$  and  $2 \pm 1.8$  nm, respectively. Meanwhile, those of AgNPs in E1 and E5 were  $23 \pm 5.5$  and  $25 \pm 8.7$  nm, respectively (Fig. 4(f) and 4(h)).

The TEM image (Fig. 4) reveals the presence of several organic layers surrounding the AgNP surface. In particular, most of the particles in TEM images do not physically in contact with each other but appear to be separated by organic layers. Therefore, the TEM image clearly shows the AgNPs layer with the organic layers. Organic layers (including alkaloids, phenolic compounds, terpenoids, enzymes, co-enzymes, proteins, sugars, etc.) facilitated the reduction of  $\text{Ag}^+$  ions and also stabilized the surface of the resulting AgNP [47-49]. Correlation between the TEM image and the color of the extract solution (Fig. 1) was clearly related to the color concentration of the solution. The color of the E extract solution is relatively more concentrated than the color of

the W extract solution. The difference in the concentration of this solution shows that E solvent dissolved more organic matter contained in *L. camara* leaves than the W solvent did (including chlorophyll in Fig. 3(b)). Therefore, the organic layer shown in the TEM image produced from the E solvent is more clearly seen than those produced from the W solvent.

### Heavy Metal Ions Sensing Studies

Test results of the colorimetric detection tests for heavy metals are presented in Fig. 5. The color change was observed in all of the Ag-extract solutions containing heavy metals. This was due to different sensitivities, such as the Ag-extract solution, which contains  $\text{Hg}^{2+}$  and  $\text{Pb}^{2+}$  ions, respectively, in the W and E solvents, the rate of the color change of the solution also varies over time.

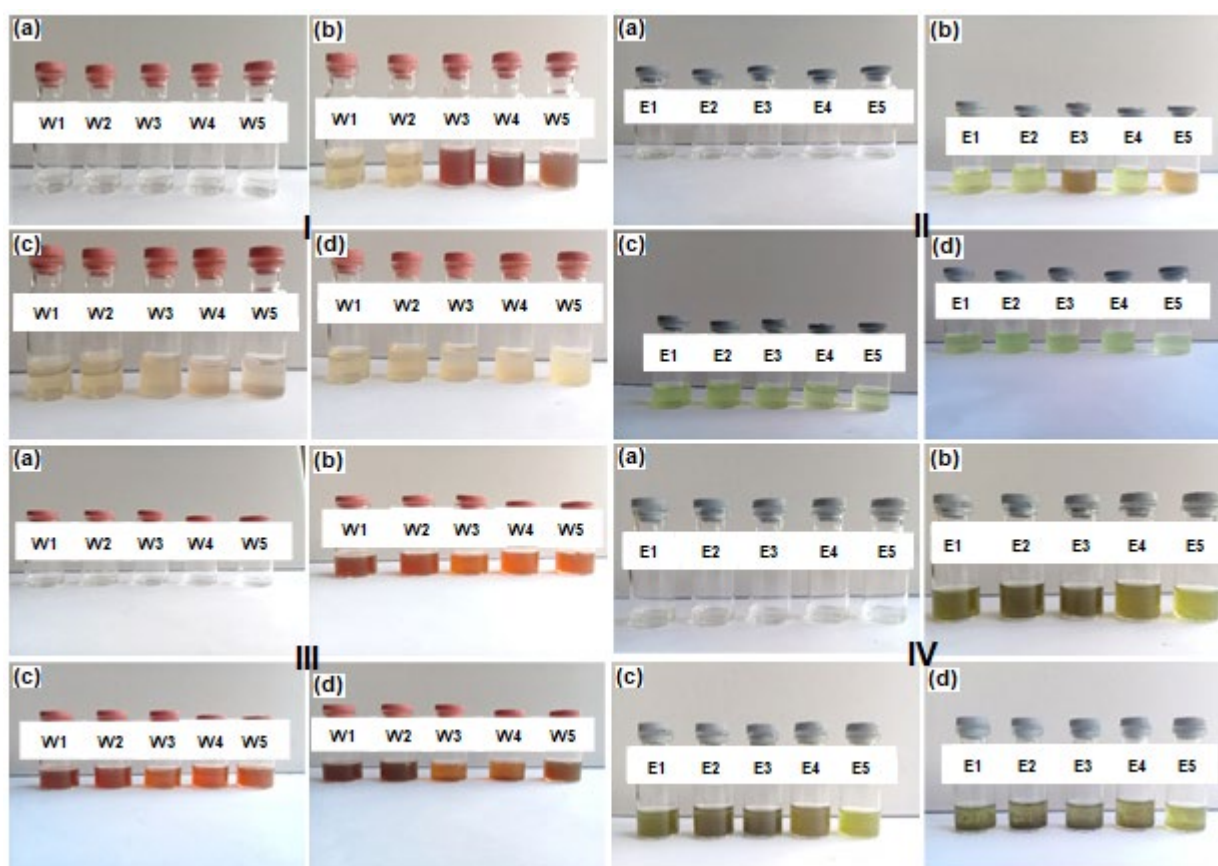


**Fig 5.** Discoloration of Ag-extract solution containing  $\text{Hg}^{2+}$  (I, II) and  $\text{Pb}^{2+}$  (III, IV) ions in each of the distilled water, W (I, III) and ethanol solvent, E (II, IV): (a) pure  $\text{AgNO}_3$  solutions, (b) at the time of addition of heavy metal solutions, (c) after 15 min, and (d) after 24 h of adding heavy metal solutions

**Table 1** Variation in AgNP size and the presence of heavy metal ions in the rate of change of Ag-extract absorption intensity for each colloid of W1-W5 and E1-E5.

Colloids	Average particle size (nm)	Detection of heavy metal ions				General explanation
		Hg <sup>2+</sup>	Cu <sup>2+</sup>	Pb <sup>2+</sup>	Mn <sup>2+</sup>	
W1	1.6	+	+	-	-	<b>Hg<sup>2+</sup></b> : absorption intensity was decreased, and the peak of the Ag spectrum was disappeared (very fast, W1 and W2 = 30 sec; W3, W4, and W5 = 30 min). <b>Cu<sup>2+</sup></b> : absorption intensity was decreased when the addition of the heavy metal solution was left up to 15 min, but it still showed a peak in the Ag spectrum and only W3 that had no peak. After 24 h of immersion, the peak of the Ag spectrum disappeared. <b>Pb<sup>2+</sup></b> and <b>Mn<sup>2+</sup></b> : generally, absorption intensity was decreased to 24 h immersion but still had a peak in the Ag spectrum.
W2	1.6	+	+	-	-	
W3	1.7	+	+	-	-	
W4	1.8	+	+	-	-	
W5	2	+	+	-	-	
E1	23	+	+	+	+	<b>Hg<sup>2+</sup></b> : absorption intensity was decreased, and the peak of the Ag spectrum was disappeared (very fast, W1 and W2 = 30 sec; W3, W4, and W5 = 30 min). <b>Cu<sup>2+</sup></b> : in general, the intensity of absorption was increased when compared to the absence of Cu ions, but the peak of the Ag spectrum was disappeared when a heavy metal solution was added for up to 24 h. <b>Pb<sup>2+</sup></b> : at the beginning of adding a heavy metal solution, all absorption intensities were increased the peak of the Ag spectrum was not observed. After 15 min and 24 h, the absorption intensity was dropped, and the peak of the Ag spectrum was not observed. <b>Mn<sup>2+</sup></b> : intensity of absorption was decreased up to 24 h of immersion, and the peak of the Ag spectrum was not observed.

It was observed that the Ag-extract solution changed color immediately after the addition of aqueous Hg<sup>2+</sup>. The color difference was quite significant compared to that without Hg<sup>2+</sup> ions, where W1 and W2 showed light brown color while W3, W4, and W5 showed brown color. After being left for 15 min, all solutions had the same color as W1 and W2, even after 24 h of immersion (Fig. 5I). The same result was shown by Ag-extract (E), where the color changed immediately after the addition of the Hg solution. In this case, E1, E2, and E4 are light green, while E3 and E5 are brown. A different result was shown by Amirjani and Haghshenas [13], where the color of the solution changed from blue to purple due to the formation of silver nano triangles functionalized by citrate. However, after 15 min, the color of the solution

became the same. They all turned light green, even after being left for 24 h (Fig. 5II). Similar results were obtained by other researchers for the interaction of metal ions with green synthesized AgNPs [50-51]. Damir et al. [52] also reported that the *L. camara* leaf extract containing AgNPs changed color from brown to transparent after the addition of a Hg<sup>2+</sup> ion solution, but no color change was observed with the addition of Zn<sup>2+</sup>, Cr<sup>3+</sup>, Cd<sup>2+</sup>, Fe<sup>2+</sup>, and Pb<sup>2+</sup> ions. A similar result was also observed by Alzahrani [12], who reported that the onion extract solution containing AgNPs became transparent after the addition of Hg<sup>2+</sup> ion solution, whereas the addition of Zn<sup>2+</sup>, Co<sup>2+</sup>, Cd<sup>2+</sup>, Cu<sup>2+</sup>, Ni<sup>2+</sup>, and Mn<sup>2+</sup> ions did not change the color.

Different results were observed for Ag-extracts, which were added with Pb(II) (Fig. 5III, IV). Visually, the color of the Ag-extract at the time of Pb addition and after 15 minutes showed a relatively similar brown. W1 and W2 are relatively darker than W3, W4, and W5. After 24 h, the five extracts became darker than before. On the other hand, in E solvent, it was noted that the extract color at the time of the Pb addition and after 15 min was relatively the same, namely light green E5. After 24 h, the colors of the five extracts were relatively similar and lighter than before.

The decreased color intensity of the solution could be explained as follows. Initially, the stabilizing agents derived from leaf extracts surrounded AgNPs to produce

nano-sized particles, and no agglomeration occurred. The addition of Ag-extract to the heavy metal solutions caused these heavy metal ions to be directly adsorbed and attached to the surface of AgNPs. As a result, the stabilizing agents from the extract were removed from the AgNP's surface. Over time, this adsorption causes more heavy metal ions to surround the AgNPs surface, and more stabilizing agents are removed from the AgNPs surface. The increase in heavy metal ions surrounding the surface of AgNPs caused aggregation, which in turn caused the color intensity of the solution to decrease [50-51,53]. Color changes observed after Ag-extracts containing heavy metal ions were analyzed using a UV-vis spectrophotometer and are presented in Fig. 6.

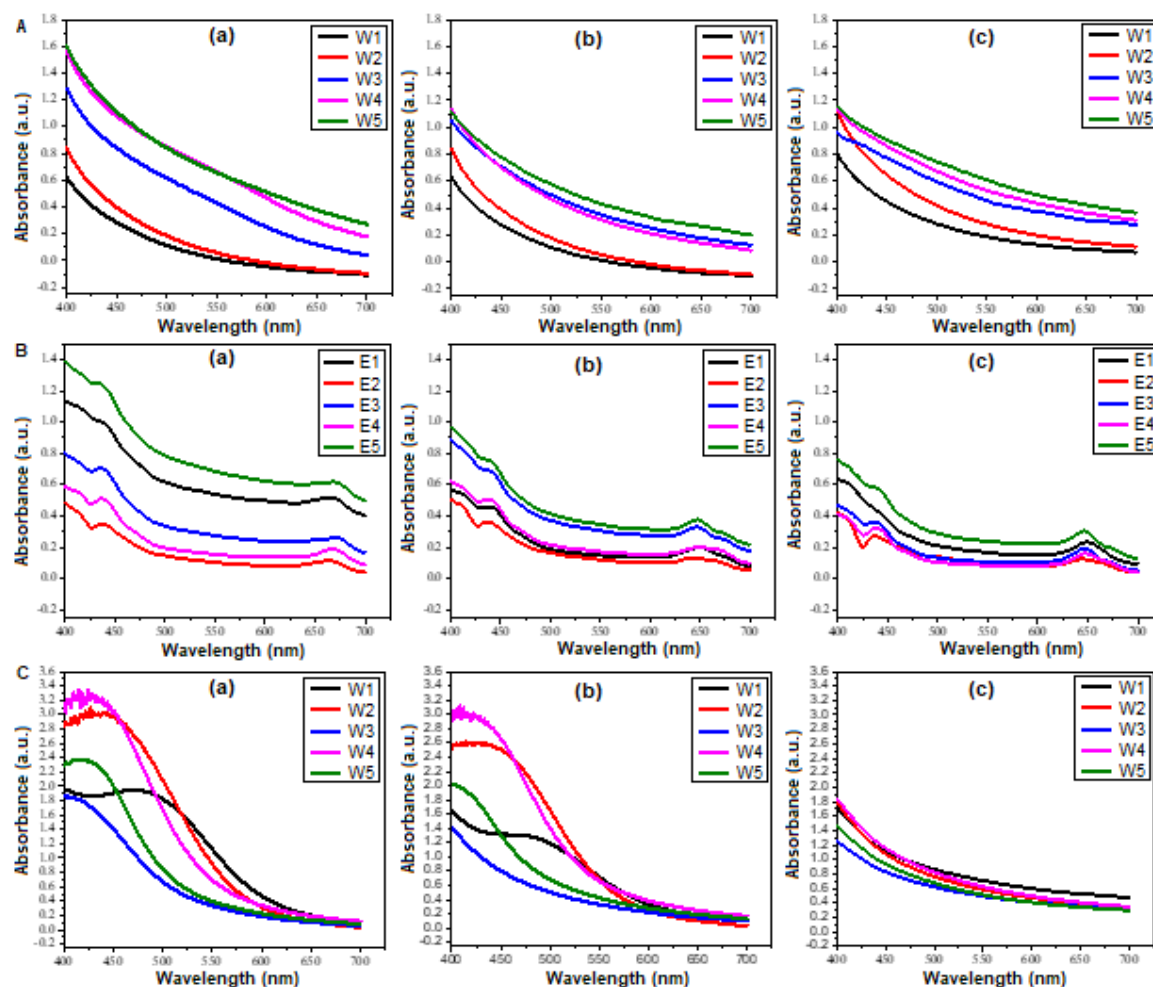


**Fig 6.** The UV-Vis absorption spectrum of AgNPs in extract solutions containing  $Hg^{2+}$  (A, B),  $Cu^{2+}$  (C, D),  $Pb^{2+}$  (E, F), and  $Mn^{2+}$  (G, H) ions in each distilled water, W (A, C, E, G) and ethanol, E (B, D, F, H) solvent: (a) at the time of heavy metal solutions addition, (b) after 15 min, and (c) after 24 h of heavy metal solutions addition

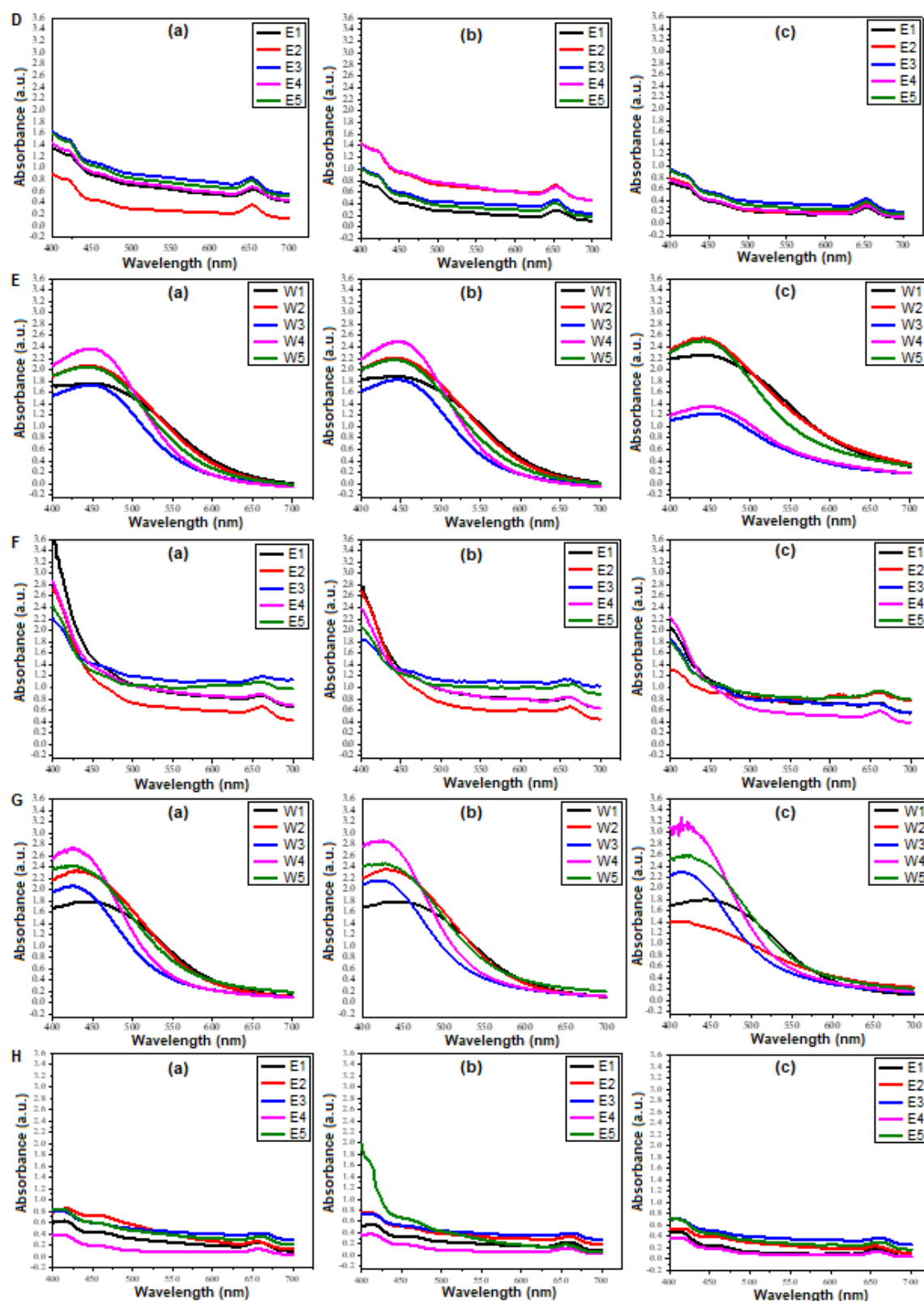


**Fig 6.** The UV-Vis absorption spectrum of AgNPs in extract solutions containing  $\text{Hg}^{2+}$  (A, B),  $\text{Cu}^{2+}$  (C, D),  $\text{Pb}^{2+}$  (E, F), and  $\text{Mn}^{2+}$  (G, H) ions in each distilled water, W (A, C, E, G) and ethanol, E (B, D, F, H) solvent: (a) at the time of heavy metal solutions addition, (b) after 15 min, and (c) after 24 h of heavy metal solutions addition (Continued)

Based on the UV-vis spectrum, it was revealed that the peak spectrum of AgNPs containing  $\text{Hg}^{2+}$  ions was missing. In addition, the absorption intensity of the solution was also relatively reduced compared to those without  $\text{Hg}^{2+}$  ions. The decrease was quite consistent from W1 to W5. This could be related to the intensity of AgNPs without  $\text{Hg}^{2+}$  ions, where the concentration of Ag at W1 is lower than W2 and so on. It was reasonable because the average size of AgNPs on W1 was relatively smaller than on W2 and so on, so  $\text{Hg}^{2+}$  ions covered the larger surface area of AgNPs and caused the absorption intensity to decrease faster. The opposite result was shown by W2 and so on because it had a relatively larger AgNPs size. Ag-extract from distilled water containing  $\text{Hg}^{2+}$  ions experienced the fastest color change, namely W1 and W2 at 30 sec while W3, W4, W5 at 30 min. This decrease in color intensity is shown in Fig. 5A and 5B. This indicated that Ag-extract could be used to detect the presence of  $\text{Hg}^{2+}$  ions in aqueous solutions ("+" sign in Table 1).

Different observations were produced by the UV-Vis AgNPs absorption spectrum after the addition of Pb solution. In general, the peak intensity of the AgNPs spectrum containing  $\text{Pb}^{2+}$  ions was decreased, but this decrease did not eliminate the peak of the AgNPs spectrum ("- " sign in Table 1). The same result was also shown by other heavy metal ions, namely Cu and Mn but with different reduction rates. The time required for these three heavy metal ions to be adsorbed on the AgNPs surface was relatively longer, which was different from that shown by the  $\text{Hg}^{2+}$  ion with the order of  $\text{Hg}^{2+} > \text{Mn}^{2+} > \text{Cu}^{2+} > \text{Pb}^{2+}$  (Table 1). Unlike  $\text{Hg}^{2+}$  ions, these three ions did not show a direct relationship between AgNPs size and the decreased absorption intensity. Despite its relatively smaller particle size, it did not show a greater decrease in absorption. This information indicated that the Ag-extract from *L. camara* using W solvent was very sensitive in detecting the presence of  $\text{Hg}^{2+}$  ions in an aqueous solution. Therefore, this method is selective enough to detect the presence of metal ions in a water sample.

The results of this study indicated that the analytical performance of this method could detect biomolecular interactions directly without labeling. In addition, it was relatively easy to use and sensitive in detecting and

identifying biomolecules so that different biochemical interactions could be monitored [54].

## ■ CONCLUSION

An eco-friendly and cost-effective protocol for the synthesis of AgNPs by utilizing renewable natural resources of *L. camara* fresh leaves was proposed. The results showed that the extracts produced using water and ethanol solvents could be used as reducing agents and capping agents to produce AgNPs. Ag-extract could be used as a sensor to detect the presence of  $\text{Hg}^{2+}$ ,  $\text{Cu}^{2+}$ ,  $\text{Pb}^{2+}$ , and  $\text{Mn}^{2+}$  in aqueous solutions. However, water solvent is more sensitive in detecting  $\text{Hg}^{2+}$  and  $\text{Cu}^{2+}$ . The order of sensitivity of the Ag-extract sensor in detecting the presence of heavy metal ions in an aqueous solution was  $\text{Hg}^{2+} > \text{Mn}^{2+} > \text{Cu}^{2+} > \text{Pb}^{2+}$ .

## ■ ACKNOWLEDGMENTS

The author would like to thank Sam Ratulangi University for its financial support through the RTUU research scheme from PNPB funds with contract number 901/UN12.13/LT/2018.

## ■ AUTHOR CONTRIBUTIONS

Conceptualization of the presented idea, H.F.A. (Henry F. Aritonang); methodology, H.F.A. and T.K. (Talita Kojong); fabricated the sample and data curation, H.F.A. and T.K., and H.K. (Harry Koleangan); writing-original draft preparation, H.F.A., T.K., H.K., and A.D.W. (Audy D. Wuntu); writing-review and editing, H.F.A., T.K., H.K., A.D.W. All authors have read and agreed to the published version of the manuscript.

## ■ REFERENCES

- [1] Briffa, J., Sinagra, E., and Blundell, R., 2020, Heavy metal pollution in the environment and their toxicological effects on humans, *Heliyon*, 6 (9), e04691.
- [2] Ali, H., Khan, E., and Ilahi, I., 2019, Environmental chemistry and ecotoxicology of hazardous heavy metals: Environmental persistence, toxicity, and bioaccumulation, *J. Chem.*, 2019, 6730305.
- [3] Massadeh, A.M., El-Rjoob, A.W.O., and Gharaibeh, S.A., 2020, Analysis of selected heavy metals in tap

- water by inductively coupled plasma-optical emission spectrometry after pre-concentration using Chelex-100 ion exchange resin, *Water Air Soil Pollut.*, 231 (5), 243.
- [4] Da Le, N., Hoang, T.T.H., Phung, V.P., Nguyen, T.L., Duong, T.T., Dinh, L.M., Pham, T.M.H., Phung, T.X.B., Nguyen, T.D., Duong, T.N., Le, T.M.H., Le, P.T., and Le, T.P.Q., 2021, Trace metal element analysis in some seafood in the coastal zone of the Red River (Ba Lat Estuary, Vietnam) by green sample preparation and inductively coupled plasma-mass spectrometry (ICP-MS), *J. Anal. Methods Chem.*, 2021, 6649362.
- [5] Adugna, E., Hymete, A., Birhanu, G., and Ashenef, A., 2020, Determination of some heavy metals in honey from different regions of Ethiopia, *Cogent Food Agric.*, 6 (1), 1764182.
- [6] Raicopol, M.D., Pandeale, A.M., Dascălu, C., Vasile, E., Hanganu, A., Vasile, G.G., Bugean, I.G., Pirvu, C., Stanciu, G., and Buica, G.O., 2020, Improving the voltammetric determination of Hg(II): A comparison between ligand-modified glassy carbon and electrochemically reduced graphene oxide electrodes, *Sensors*, 20 (23), 6799.
- [7] López-García, I., Marín-Hernández, J.J., and Hernández-Córdoba, M., 2020, Speciation of chromium in waters using dispersive micro-solid phase extraction with magnetic ferrite and graphite furnace atomic absorption spectrometry, *Sci Rep.*, 10 (1), 5268.
- [8] Zhang, H., Antonangelo, J., and Penn, C., 2021, Development of a rapid field testing method for metals in horizontal directional drilling residuals with XRF sensor, *Sci Rep.*, 11 (1), 3901.
- [9] Senila, M., Cadar, O., Senila, L., Böringer, S., Seaudeau-Pirouley, K., Ruiu, A., and Lacroix-Desmazes, P., 2020, Performance parameters of inductively coupled plasma optical emission spectrometry and graphite furnace atomic absorption spectrometry techniques for Pd and Pt determination in automotive catalysts, *Materials*, 13 (22), 5136.
- [10] Feng, X., Zhang, H., and Yu, P., 2020, X-ray fluorescence application in food, feed, and agricultural science: A critical review, *Crit. Rev. Food Sci. Nutr.*, 0 (0), 1–11.
- [11] Singh, C., Kumar, J., Kumar, P., Chauhan, B.S., Tiwari, K.N., Mishra, S.K., Srikrishna, S., Saini, R., Nath, G., and Singh, J., 2019, Green synthesis of silver nanoparticles using aqueous leaf extract of *Premna integrifolia* (L.) rich in polyphenols and evaluation of their antioxidant, antibacterial and cytotoxic activity, *Biotechnol. Biotechnol. Equip.*, 33 (1), 359–371.
- [12] Alzahrani, E., 2020, Colorimetric detection based on localized surface plasmon resonance optical characteristics for sensing of mercury using green-synthesized silver nanoparticles, *J. Anal. Methods Chem.*, 2020, 6026312.
- [13] Amirjani, A., and Haghshenas, D.F., 2018, Ag nanostructures as the surface plasmon resonance (SPR)-based sensors: A mechanistic study with an emphasis on heavy metallic ions detection, *Sens. Actuators, B*, 273, 1768–1779.
- [14] Patel, K., Bhamore, J.R., Park, T.J., and Kailasa, S.K., 2018, Selective and sensitive colorimetric recognition of Ba<sup>2+</sup> ion using guanine-functionalized silver nanoparticles, *ChemistrySelect*, 3 (36), 10182–10187.
- [15] Mehta, V.N., Rohit, J.V., and Kailasa, S.K., 2016, Functionalization of silver nanoparticles with 5-sulfoanthranilic acid dithiocarbamate for selective colorimetric detection of Mn<sup>2+</sup> and Cd<sup>2+</sup> ions, *New J. Chem.*, 40, 4566–4574.
- [16] Amirjani, A., Bagheri, M., Heydari, M., and Hesaraki, S., 2016, Colorimetric determination of Timolol concentration based on localized surface plasmon resonance of silver nanoparticles, *Nanotechnology*, 27 (37), 375503.
- [17] Modi, R.P., Mehta, V.N., and Kailasa S.K., 2014, Bifunctionalization of silver nanoparticles with 6-mercaptopyridine and melamine for simultaneous colorimetric sensing of Cr<sup>3+</sup> and Ba<sup>2+</sup> ions, *Sens. Actuators, B*, 195, 562–571.

- [18] Kailasa, S.K., Chandel, M., Mehta, V.N., and Park, T.J., 2018, Influence of ligand chemistry on silver nanoparticles for colorimetric detection of Cr<sup>3+</sup> and Hg<sup>2+</sup> ions, *Spectrochim. Acta, Part A*, 195, 120–127.
- [19] Koochak, N.N., Rahbarimehr, E., Amirjani, A., and Haghshenas, D.F., 2021, Detection of cobalt ion based on surface plasmon resonance of L-cysteine functionalized silver nanotriangles, *Plasmonics*, 16 (2), 315–322.
- [20] Amirjani, A., and Fatmehsari, D.H., 2018, Colorimetric detection of ammonia using smartphones based on localized surface plasmon resonance of silver nanoparticles, *Talanta*, 176, 242–246.
- [21] Awad, M.A., Hendi, A.A., Ortashi, K.M.O., Alotaibi, R.A., and Sharafeldin, M.S., 2016, Characterization of silver nanoparticles prepared by wet chemical method and their antibacterial and cytotoxicity activities, *Trop. J. Pharm. Res.*, 15 (4), 679–685.
- [22] Islam, T., Hasan, M.M., Awal, A., Nurunnabi, Md., and Ahammad, A.J.S., 2020, Metal nanoparticles for electrochemical sensing: Progress and challenges in the clinical transition of point-of-care testing, *Molecules*, 25 (24), 5787–5842.
- [23] Salleh, M.S.N., Ali, R.R., Shameli, K., Hamzah, M.Y., and Chan, J.Z., 2020, Silver nanoparticles on pullulan derived via gamma irradiation method: a preliminary analysis, *IOP Conf. Ser.: Mater. Sci. Eng.*, 808, 012030.
- [24] Moglia, I., Santiago, M., Soler, M., and Olivera-Nappa, A., 2020, Silver nanoparticle synthesis in human ferritin by photochemical reduction, *J. Inorg. Biochem.*, 206, 111016.
- [25] Saha, S., Ghosh, M., Dutta, B., and Chowdhury, J., 2016, Self-assembly of silver nanocolloids in the Langmuir–Blodgett film of stearic acid: Evidence of an efficient SERS sensing platform, *J. Raman Spectrosc.*, 47, 168–176.
- [26] Afreen, A., Ahmed, R., Mehboob, S., Tariq, M., Alghamdi, H.A., Zahid, A.A., Ali, I., Malik, K., and Hasan, A., 2020, Phytochemical-assisted biosynthesis of silver nanoparticles from *Ajuga bracteosa* for biomedical applications, *Mater. Res. Express*, 7(7) 075404
- [27] Bahrulolum, H., Nooraei, S., Javanshir, N., Tarrahimofrad, H., Mirbagheri, V.S., Easton, A.J., and Ahmadian, G., 2021, Green synthesis of metal nanoparticles using microorganisms and their application in the agrifood sector, *J. Nanobiotechnol.*, 19 (1), 86.
- [28] Mondal, A.H., Yadav, D., Mitra, S., and Mukhopadhyay, K., 2020, Biosynthesis of silver nanoparticles using culture supernatant of *Shewanella* sp. ARY1 and their antibacterial activity, *Int. J. Nanomed.*, 15, 8295–8310.
- [29] Aritonang, H.F., Onggo, D., Ciptati, C., and Radiman, C.L., 2015, Insertion of platinum particles in bacterial cellulose membranes from PtCl<sub>4</sub> and H<sub>2</sub>PtCl<sub>6</sub> precursors, *Macromol. Symp.*, 353 (1), 55–61.
- [30] Aritonang, H.F., Kamea, O.E., Koleangan, H., and Wuntu, A.D., 2020, Biotemplated synthesis of Ag-ZnO nanoparticles/bacterial cellulose nanocomposites for photocatalysis application, *Polym.-Plast. Technol. Mater.*, 59 (12), 1292–1299.
- [31] Aritonang, H.F., Koleangan, H., and Wuntu, A.D., 2019, Synthesis of silver nanoparticles using aqueous extract of medicinal plants' (*Impatiens balsamina* and *Lantana camara*) fresh leaves and analysis of antimicrobial activity, *Int. J. Microbiol.*, 2019, 8642303.
- [32] Jadoun, S., Arif, R., Jangid, N.K., and Meena, R.K., 2020, Green synthesis of nanoparticles using plant extracts: A review, *Environ. Chem. Lett.*, 19 (1), 355–374.
- [33] Castillo-Henríquez, L., Alfaro-Aguilar, K., Ugalde-Álvarez, J., Vega-Fernández, L., Montes de Oca-Vásquez, G., and Vega-Baudrit, J.R., 2020, Green synthesis of gold and silver nanoparticles from plant extracts and their possible applications as antimicrobial agents in the agricultural area, *Nanomaterials*, 10 (9), 1763–1786.
- [34] Vanlalveni, C., Lallianrawna, S., Biswas, A., Selvaraj, M., Changmai, B., and Rokhum, S.L., 2021, Green synthesis of silver nanoparticles using plant extracts and their antimicrobial activities: A review of recent literature, *RSC Adv.*, 11 (5), 2804–2837.

- [35] Ajitha, B., Reddy, Y.A.K., Shameer, S., Rajesh, K.M., Suneetha, Y., and Reddy, P.S., 2015, *Lantana camara* leaf extract mediated silver nanoparticles: Antibacterial, green catalyst, *J. Photochem. Photobiol., B*, 149, 84–92.
- [36] Sharifi-Rad, M., Pohl, P., Epifano, F., and Álvarez-Suarez, J.M., 2020, Green synthesis of silver nanoparticles using *Astragalus tribuloides* Delile. root extract: Characterization, antioxidant, antibacterial, and anti-inflammatory activities, *Nanomaterials*, 10 (12), 2383.
- [37] Zarei, Z., Razmjoue, D., and Karimi, J., 2020, Green synthesis of silver nanoparticles from *Caralluma tuberculata* extract and its antibacterial activity, *J. Inorg. Organomet. Polym. Mater.*, 30 (11), 4606–4614.
- [38] Seifipour, R., Nozari, M., and Pishkar, L., 2020, Green synthesis of silver nanoparticles using *Tragopogon collinus* leaf extract and study of their antibacterial effects, *J. Inorg. Organomet. Polym. Mater.*, 30 (8), 2926–2936.
- [39] Ahmad, M.A., Salmiati, S., Marpongahtun, M., Salim, M.R., Lolo, J.A., and Syafiuddin, A., 2020, Green synthesis of silver nanoparticles using *Muntingia calabura* leaf extract and evaluation of antibacterial activities, *Biointerface Res. Appl. Chem.*, 10 (5), 6253–6261.
- [40] Mikhailova, E.O., 2020, Silver nanoparticles: Mechanism of action and probable bio-application, *J. Funct. Biomater.*, 11 (4), 84.
- [41] Sangule, O.T., 2020, Green synthesis of silver nanoparticles from leaf extract of *Lantana camara*, characterization and antimicrobial activity, *Int. J. Recent Sci. Res.*, 11 (4), 38297–38300.
- [42] Palei, N.N., Ramu, S., Vijaya, V., Thamizhvanan, K., and Balaji, A., 2020, Green synthesis of silver nanoparticles using leaf extract of *Lantana camara* and its antimicrobial activity, *Int. J. Green Pharm.*, 14 (2), 155–161.
- [43] Kumar, B., Smita, K., and Cumbal, L., 2016, Biosynthesis of silver nanoparticles using *Lantana camara* flower extract and its application, *J. Sol-Gel Sci. Technol.*, 78 (2), 285–292.
- [44] Shriniwas, P.P., and Subhash, T.K., 2017, Antioxidant, antibacterial and cytotoxic potential of silver nanoparticles synthesized using terpenes rich extract of *Lantana camara* L. leaves, *Biochem. Biophys. Rep.*, 10, 76–81.
- [45] Dubey, D., and Pandhy, R.N., 2013, Antibacterial activity of *Lantana camara* L. against multidrug resistant pathogens from ICU patients of a teaching hospital, *J. Herb. Med.*, 3 (2), 65–75.
- [46] Ajitha, B., Reddy, Y.A.K., and Reddy, P.S., 2015, Green synthesis and characterization of silver nanoparticles using *Lantana camara* leaf extract, *Mater. Sci. Eng., C*, 49, 373–381.
- [47] Shaik, M.R., Khan, M., Kuniyil, M., Al-Warthan, A., Alkathlan, H.Z., Siddiqui, M.R.H., Shaik, J.P., Ahmed, A., Mahmood, A., Khan, M., and Adil, S.F., 2018, Plant-extract-assisted green synthesis of silver nanoparticles using *Origanum vulgare* L. extract and their microbicidal activities, *Sustainability*, 10 (4), 913.
- [48] Mittal, A.K., Chisti, Y., and Banerjee, U.C., 2013, Synthesis of metallic nanoparticles using plant extracts, *Biotechnol. Adv.*, 31 (2), 346–356.
- [49] Jha, A.K., Prasad, K., Prasad, K., and Kulkarni, A.R., 2009, Plant system: Nature's nanofactory, *Colloids Surf., B*, 73 (2), 219–223.
- [50] Maiti, S., Barman, G., and Laha, J.K., 2016, Detection of heavy metals ( $\text{Cu}^{+2}$ ,  $\text{Hg}^{+2}$ ) by biosynthesized silver nanoparticles, *Appl. Nanosci.*, 6 (4), 529–538.
- [51] Karthiga, D., and Anthony, S.P., 2013, Selective colorimetric sensing of toxic metal cations by green synthesized silver nanoparticles over a wide pH range, *RSC Adv.*, 3 (37), 16765–16774.
- [52] Demir, D., Bölgen, N., and Vaseashta, A., 2018, “Green Synthesis of Silver Nanoparticles Using *Lantana camara* Leaf Extract and Their Use as Mercury(II) Ion Sensor” in *Advanced Nanotechnologies for Detection and Defence against CBRN Agents. NATO Science for Peace and Security Series B: Physics and Biophysics*, Eds. Petkov, P., Tsiulyanu, D., Popov, C., and Kulisch, W., Springer, Dordrecht, 427–433.

- [53] Ihsan, M., Niaz, A., Rahim, A., Zaman, M.I., Arain, M.B., Sirajuddin, Sharif, T., and Najeeb, M., 2015, Biologically synthesized silver nanoparticle-based colorimetric sensor for the selective detection of  $Zn^{2+}$ , *RSC Adv.*, 5 (111), 91158–91165.
- [54] Daghestani, H.N., and Day, B.W., 2010, Theory and applications of surface plasmon resonance, resonant mirror, resonant waveguide grating, and dual polarization interferometry biosensors, *Sensors*, 10 (11), 9630–9646.